Structure and optical properties of two types of F centre in BaFBr

1992 J. Phys.: Condens. Matter 4 3001

(http://iopscience.iop.org/0953-8984/4/11/024)

J. Phys.: Condens. Matter 4 (1992) 3001–3013. Printed in the UK

Structure and optical properties of two types of F centre in BaFBr

F K Koschnick†, Th Hangleiter†, J-M Spaeth†, and R S Eachus‡

† University of Paderborn, Warburger Strasse 100, 4790 Paderborn, Federal Republic of Germany

‡ Eastman Kodak Company, Research Laboratories, Rochester, New York 14650-2021, USA

Received 23 October 1991

Abstract. A detailed investigation of the optical absorption and emission bands from the two types of F centre in BaFBr is reported, using optical, magneto-optical, and optically detected electron paramagnetic resonance and electron nuclear double resonance (ENDOR) techniques. With conventional ENDOR, the superhyperfine interactions of the $F(Br^-)$ centre are investigated in detail. It was found from the luminescence experiments that the two types of F centre are spatially correlated when they are created by x-irradiation in qualitative agreement with the observation of cross relaxation effects, as reported elsewhere.

1. Introduction

Europium-doped BaFBr is an important material for storage phosphor. It is generally agreed that the stable image produced by the absorption of x-radiation is composed of trapped electron and hole centres. BaFBr, like PbFCl, has the matlockite structure which consists of layers in the sequence F^-–Ba^{2+}–Br^-–Br^-–Ba^{2+}–F^- perpendicular to a c-axis. The crystal has the tetragonal space group $P4/nmm$ (Beck 1979, Liebig 1977). The trapped electron centres involved in the imaging are F centres which, in BaFBr, have two possible structures. An electron is either trapped in a bromide vacancy to give $F(Br^-)$ or in a fluoride vacancy giving $F(F^-)$. These centres have C_{4v} and D_{2d} symmetries, respectively (see figure 1). In SrFBr and BaFCl, both types of F centre have been produced by additive coloration and their structures have been investigated in detail by electron nuclear double resonance (ENDOR) techniques (Bauer 1983, Niklas 1983). A similar detailed investigation has not been reported for BaFBr. In particular, all the relevant optical properties of both types of F centre are not known precisely. There is also some disagreement with regard to the contribution of $F(F^-)$ centres to the photostimulation process in europium-doped material. This process leads to the read-out of the stored image from the storage phosphor in practice (Sonoda 1983, Takahashi 1985, Seggern 1988a,b). The disagreement is largely due to insufficient knowledge of all the optical absorption transitions of the two types of F centre. It is not straightforward to obtain these data from optical measurements alone. However, applying magneto-optical techniques together with optically detected electron paramagnetic resonance (ODEPR) it is possible to obtain this information.

0953-8984/92/113001+13$04.50

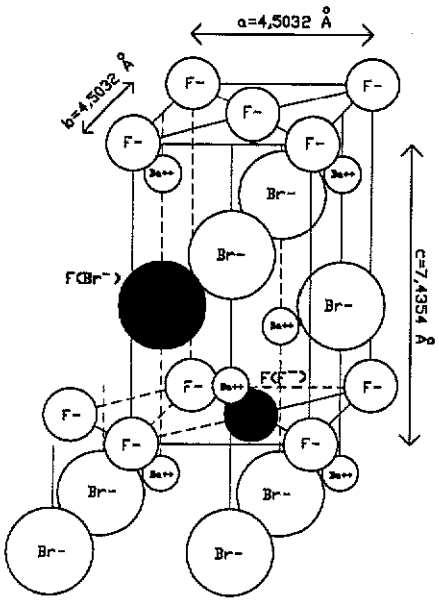

Figure 1. The structure of BaFBr and schematic representation of the two F centres.

It is the purpose of this paper to investigate the structures and the optical properties of both types of F centres. In view of the application of BaFBr as a phosphor storage material, it is also important to investigate whether the F centres produced by x-irradiation at room temperature have the same properties as those generated by additive coloration.

2. Experimental details

2.1. Crystal growth and sample preparation

Before crystal growth BaF_2 (Merck, grade optipur) was purified by zone refining in vitreous carbon crucibles and $BaBr_2$ (prepared by G McDugle from Eastman Kodak) was dried under vacuum and treated with $SiBr_4$ to remove oxygen. Single crystals were grown in graphite crucibles by the Bridgman–Stockbarger method from a stoichiometric mixture of BaF_2 and $BaBr_2$ under an argon atmosphere. Nearly transparent single crystals of excellent quality were obtained. The samples were cut with a wire saw and orientated by Laue back reflection. F centres were produced by room-temperature x-irradiation (50 kV, 40 mA, 3–10 min) or by additive coloration with the van Doorn method (van Doorn 1961). It was found from low-temperature x-irradiation that the crystals still contained oxide impurities in a concentration range of 10–100 ppm. The influence of this residual oxide on F centre production is discussed in Koschnick (1992). The properties of F centres reported here are independent of the oxide content of the crystals. Upon room-temperature x-irradiation, isolated F centres are produced (Koschnick 1992).

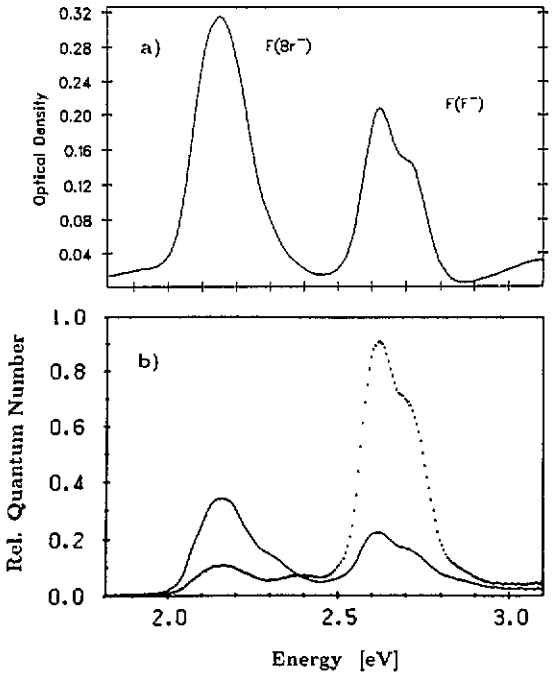

Figure 2. (*a*) Optical absorption of $F(Br^-)$ and $F(F^-)$ centres for $\boldsymbol{E} \perp c$, $T = 10$ K. (*b*) Excitation spectra of the luminescence of the $F(F^-)$ (dotted curve) and $F(Br^-)$ centres for $\boldsymbol{E} \perp c$, $T = 10$ K.

2.2. Optical and magneto-optical measurements, electron paramagnetic resonance

Optical absorption measurements were performed with a computer-controlled single-beam spectrometer with a 0.25 m double monochromator (Spex) and various lamps and detectors. Detection in the infrared range was limited at 1.7 μm (Ge detector, North-coast). The luminescence and its excitation spectra were corrected for the spectral response of the spectrometer. The magnetic circular dichroism of the absorption (MCDA) which is the differential absorption of right and left circularly polarized light and the ODEPR and ODENDOR were measured in a custom-built, computer-controlled spectrometer. The MCDA is proportional to the spin polarization of the ground state of a paramagnetic defect. ODEPR is measured as a microwave-induced change in the MCDA (Ahlers 1983) at 24 GHz at 1.5 or 4.2 K. For ODENDOR an additional RF field is applied to the sample (Hofmann 1984). Conventional EPR and ENDOR were also measured using a computer-controlled homodyne spectrometer operating at 9.5 GHz at temperatures between 40 and 300 K (Hoentzsch 1978). The ENDOR spectra were treated with digital filters and special peak-search and deconvolution algorithms to determine the frequency position of the ENDOR lines (Bromba 1979, Ziegler 1981, Niklas 1983).

3. Experimental results

3.1. Optical and magneto-optical measurements

Additively coloured BaFBr shows two absorption bands peaking at 2.15 eV and

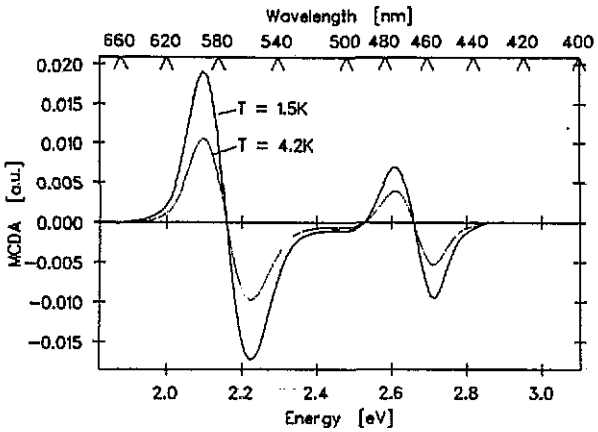

Figure 3. MCDA spectra of $F(Br^-)$ and $F(F^-)$ centres for $E \perp c$ at two temperatures, $B = 3000$ mT.

2.65 eV if the electrical vector E of the light is perpendicular to the c-axis (figure 2(a)). Both bands are superpositions of two bands. They can be decomposed into two Gaussian bands separated by 130 and 100 meV, respectively. It will be shown later that the band at 2.15 eV is the absorption of $F(Br^-)$ centres, that at 2.65 eV belongs to $F(F^-)$ centres. Both absorptions can also be created by room-temperature x-irradiation. The MCDA of a room-temperature x-irradiated crystal (figure 3) measured for $E \perp c$ shows two derivative-like structures for which the MCDA vanishes at the peak energies of the absorption bands. This is very similar to what is known from F centres in the alkali halides where the spectral shape of the MCDA is the derivative of the Gaussian absorption band (Luty 1964). It is also seen in figure 3 that the MCDA is temperature-dependent and thus due to paramagnetic centres (Henry 1968). Its magnetic field dependence for constant temperature can be explained for a defect with $g = 2$ and $S = \frac{1}{2}$, as expected for F centres.

The optical absorption spectrum for E parallel to the c-axis of a room-temperature x-irradiated crystal contains a band peaking at 2.35 eV and one at 2.52 eV (figure 4(a)). At low temperature only $F(Br^-)$centres are created with x-irradiation (Koschnick 1992). A comparison with a low-temperature x-irradiated crystal where only $F(Br^-)$ centres are formed, allows the assignment of the band at 2.52 eV to $F(Br^-)$ centres and that at 2.35 eV to $F(F^-)$ centres (see table 1). MCDA spectra could not be measured for E parallel to the c-axis. The BaFBr crystal has a strong birefringence which causes a very large dichroism for $E \parallel c$, much larger than that of the centres produced by x-irradiation, which therefore could not be measured for this geometry. The MCDA could only be measured for light propagating parallel to the c-axis and a few degrees off that direction.

Table 1. Peak energies (eV) of optical absorption and emission bands of $F(F^-)$ and $F(Br^-)$ centres in BaFBr at $T = 10$ K.

Polarization	$F(Br^-)$	$F(F^-)$
$E \perp c$	2.15, 2.3–2.8	2.65, $\approx$ 3.5
$E \parallel c$	2.58	2.38

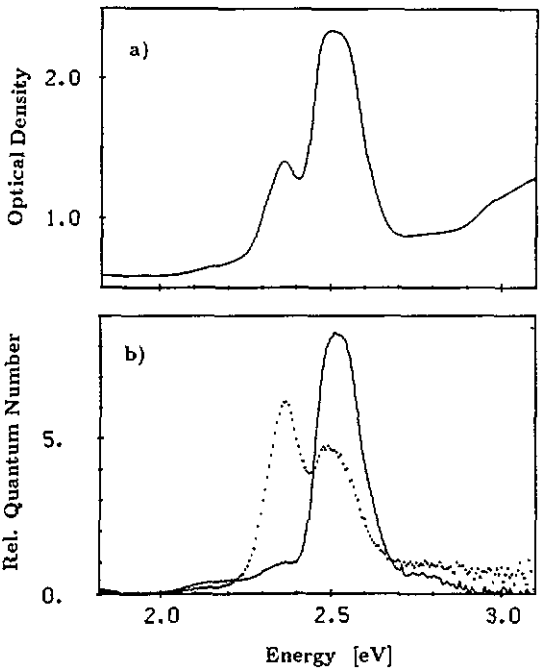

Figure 4. (*a*) Optical absorption of $F(F^-)$ and $F(Br^-)$ centres for $\boldsymbol{E} \parallel c$, $T = 10$ K. (*b*) Excitation spectra of the $F(F^-)$ (dotted curve) and $F(Br^-)$ centres for $\boldsymbol{E} \parallel c$, $T = 10$ K.

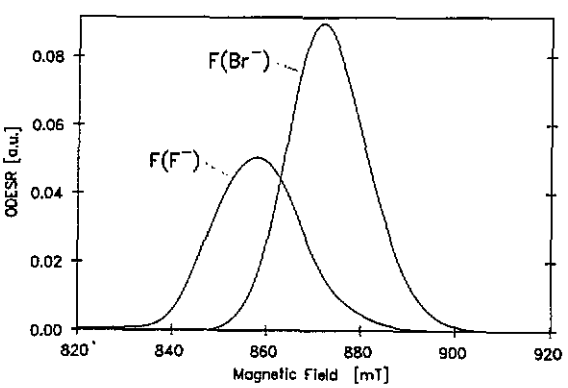

Figure 5. ODEPR spectrum of $F(F^-)$ and $F(Br^-)$ centres with $\boldsymbol{B} \parallel c$, microwave frequency 24 GHz, $T = 1.5$ K.

3.2. Optical detection of EPR and ENDOR (ODEPR and ODENDOR)

ODEPR could only be measured for the magnetic field parallel to the *c*-axis due to the large birefringence of the crystal for other orientations. Figure 5 shows the ODEPR lines measured in each of the two MCDA spectra of figure 3. The line at $g_{\parallel} = 2.0$ measured in the MCDA centred at 2.65 eV ($\boldsymbol{E} \perp c$) belongs to $F(F^-)$ centres, that at $g_{\parallel} = 1.98$ (higher field) measured in the MCDA centred at 2.15 eV to $F(Br^-)$ centres. With the MCDA technique, one measures the EPR absorption and not the derivative

that is normally obtained in conventional EPR. The identification of the two ODEPR spectra with the two centres is based on a comparison with conventional EPR and ENDOR experiments described in section 3.4. The ODEPR linewidths are broader than those observed in conventional EPR. The reasons for this are unavoidable saturation broadening effects since the ODEPR spectra had to be measured at higher microwave power levels. The ODENDOR spectrum measured in the MCDA of $F(Br^-)$ centres at $g_\parallel = 1.98$ is shown in figure 6 ($B_0 \parallel c$). It is identical to that measured with conventional detection for the same magnetic field orientation. The assignment of the ODENDOR lines to specific neighbour nuclei (the right-hand superscript denotes the shell number) is based on an analysis of the angular dependence and field shift experiments of the conventional ENDOR spectra (see section 3.4). The maximum ODENDOR effect was observed in the flanks of the ODEPR lines. Figure 7 shows the ODENDOR spectrum of $F(F^-)$ centres for $B_0 \parallel c$. The chemical identity of the nuclei causing the ENDOR lines was established by field shift measurements of their frequency positions (Seidel 1968). Unfortunately a comparison with conventional ENDOR was not possible since the low number of $F(F^-)$ centres did not allow conventional ENDOR measurements. ODENDOR is much more sensitive than conventional ENDOR. An angular dependence of the ODENDOR spectrum could not be measured because of the crystal's large birefrigence for field orientations away from the c-axis.

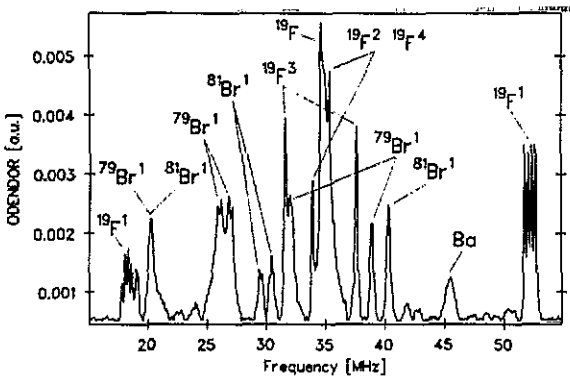

Figure 6. ODENDOR spectrum of $F(Br^-)$ centres with $B \parallel c$, $B = 890$ mT, $T = 1.5$ K.

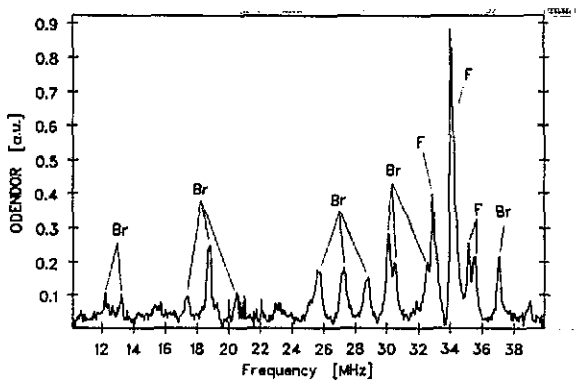

Figure 7. ODENDOR spectrum of $F(F^-)$ centres with $B \parallel c$, $B = 870$ mT, $T = 1.5$ K.

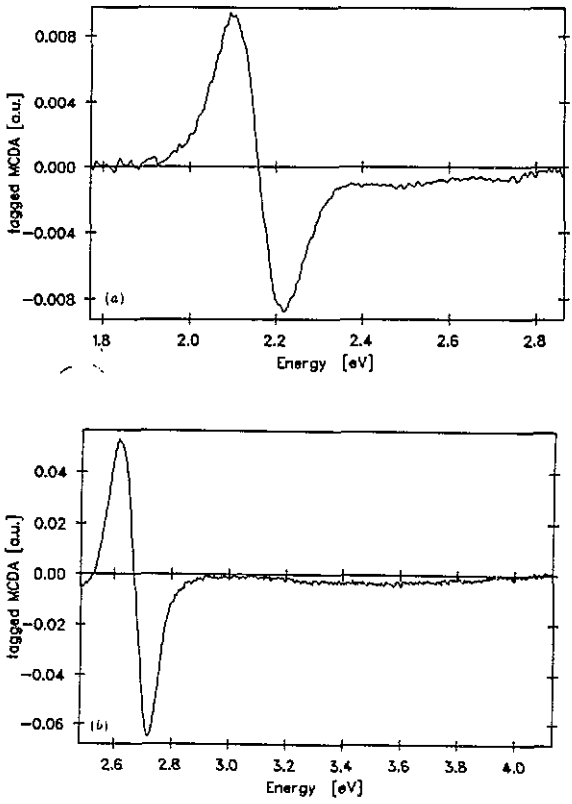

Figure 8. (*a*) MCDA tagged by the EPR of $F(Br^-)$ centres, $T = 1.5$ K. (*b*) MCDA tagged by the EPR of $F(F^-)$ centres, $T = 1.5$ K.

In additively coloured BaFBr besides the two dominant MCDA bands at 2.15 and 2.65 eV ($\boldsymbol{E} \perp c$) of $F(Br^-)$ and $F(F^-)$ centres, respectively, a broad but relatively weak MCDA band could be measured centred at about 3.5 eV. ODEPR measurements in this broad MCDA revealed that this band is a high-energy transition of the $F(F^-)$ centre. Both the g factor and the half-width as well as the spin–lattice relaxation time are the same as those measured in the MCDA band centred about 2.65 eV. By measuring the ODEPR excitation spectrum (MCDA-tagged EPR (Ahlers 1983)) in the $F(F^-)$ EPR line both optical transitions of the $F(F^-)$ centre could be reproduced (see figure 8(*b*)). In addition the $F(Br^-)$ centre has a second optical absorption for $\boldsymbol{E} \perp c$. Since this second transition overlaps with the absorptions of the $F(F^-)$ centres one has to prepare the crystals in such a way as to avoid the presence of $F(F^-)$ centres in order to measure it. This can be done by x-irradiating BaFBr at low temperatures where only $F(Br^-)$ centres are formed (Koschnick 1992). Figure 8(*a*) shows the MCDA tagged in the EPR spectrum of $F(Br^-)$ centres. Comparison with the absorption spectrum for $\boldsymbol{E} \perp c$ (figure 2(*a*)) shows that the high-energy transition of $F(Br^-)$ centres overlaps with the main absorption band of $F(F^-)$ centres.

3.3. Infrared luminescence from $F(F^-)$ and $F(Br^-)$

Figure 9 shows the two luminescence bands obtained by excitation in the absorption bands of $F(F^-)$ and $F(Br^-)$ centres. Both bands are identical for excitation with $\boldsymbol{E}$

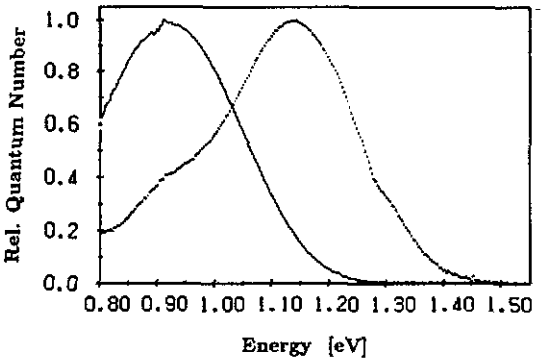

Figure 9. Luminescence spectra of $F(F^-)$ and $F(Br^-)$ centres at $T = 10$ K.

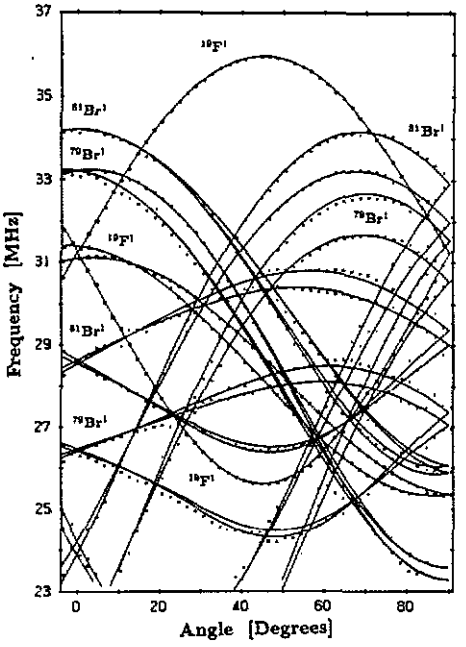

Figure 10. Angular dependence of the ENDOR spectra of $F(Br^-)$ centres for rotations with B in the a–c plane, $m_s = -\frac{1}{2}$, $B = 334$ mT, $T = 40$ K.

parallel and perpendicular to c. The luminescence from the $F(Br^-)$ centres peaks at 0.92 eV (1348 nm) and that from $F(F^-)$ at 1.14 eV (1087 nm) at 10 K. Figure 9 contains a deconvolution of the spectra into several Gaussian bands. Excitation at 2.65 eV for $E \perp c$ shows clear emissions from both $F(F^-)$ and $F(Br^-)$ (see later). The $F(Br^-)$ emission spectrally overlaps in the higher flank with that from the $F(F^-)$ centres while that of the $F(F^-)$ emission in the lower energy flank is better separated from the peak of the $F(Br^-)$ emission. The excitation spectra of the emissions from both F centres were measured for E parallel and perpendicular to c. They are shown in figures 2(b) and 4(b). Surprisingly, by exciting the $F(Br^-)$ band with light of polarization $E \parallel c$, both emissions could be observed, whereas only the $F(F^-)$ luminescence was produced by excitation in the $F(F^-)$ band. Since the excitation

spectrum for $E \perp c$ of the $F(Br^-)$ luminescence reproduces exactly the $F(F^-)$ absorption band, this effect cannot be caused by the higher optical transition (K-band) of the $F(Br^-)$ centre, or by scattering effects, or by excitation of the transition with $E \parallel c$ (i.e. misorientation of the crystal). When exciting the F bands for $E \parallel c$ (figure 4(*b*)) the emissions behave in the reverse manner. In the $F(F^-)$ band only the $F(F^-)$ emission could be excited (the small component of $F(F^-)$ underneath the excitation spectrum of the $F(Br^-)$ centre in figure 4(*b*) is due to the overlap of the two emissions at 1.14 eV—see figure 9—and could have been eliminated by numerical correction). Both of the $F(F^-)$ and $F(Br^-)$ emissions could be excited by irradiation in the $F(Br^-)$ band (figure 4(*b*)).

Table 2. SHF and quadrupole interaction constants and tensor orientations of $F(Br^-)$ centres at $T = 40$ K. (*a*) SHF interaction constants and (*b*) quadrupole interaction constants for the $^{81}Br^1$ nuclei.

(*a*)

Shell	a (MHz)	b (MHz)	b' (MHz)	ϑ (deg)	ψ (deg)	ϕ (deg)
$^{19}F^1$	31.20	6.99	−0.31	45.0	0	0
$^{81}Br^1$	50.08	3.66	1.01	126.8	180.0	225.0
$^{19}F^2$	0.87	0.46	−0.04	89.9	0	0
$^{19}F^3$	6.52	1.11	0.23	92.5	92.8	209.6
$^{19}F^4$	1.25	0.36	0	137.3	181.8	0

(*b*)

q (MHz)	q' (MHz)	ϑ (deg)	ψ (deg)	ϕ (deg)
1.05	0.75	12.7	180.0	225.0

3.4. Conventional EPR and ENDOR of $F(Br^-)$ centres

In x-irradiated BaFBr no ENDOR measurements could be done because of the low F centre concentration obtainable. The sensitivity of conventional ENDOR is much lower than that of ODENDOR for F centres which have a high oscillator strength for their optical transition. Therefore ENDOR from additively coloured crystals had to be measured. With these crystals strong EPR and ENDOR signals of $F(Br^-)$ centres were obtained. The EPR measurements showed a single line with an axial g-matrix with the principal direction parallel to the c-axis. The g-matrix can be described by the two g factors $g_\parallel = 1.98$ and $g_\perp = 1.99$. The half-width of the EPR line is about 12 mT for $B \parallel c$. The ENDOR measurements were performed at a magnetic field of $B = 334$ mT. Strong fluorine and bromine ENDOR signals were observed. ENDOR from Ba isotopes could not be observed because of the low abundance of both magnetic $^{135,137}Ba$ isotopes. Figure 10 shows the angular dependence of the ENDOR spectrum between 23 and 37 MHz for rotation of the magnetic field in the a–c plane. (The dots are the experimental line positions.) The result of the ENDOR analysis confirmed that the EPR and ENDOR signals originated from the $F(Br^-)$ centre. The ENDOR lines seen in figure 10 are due to the first ^{19}F and $^{79,81}Br$ shell. The theoretical ENDOR angular dependences calculated with the superhyperfine (SHF) and quadrupole interaction constants of table 2, which were obtained from the analysis of the spectra using the usual spin Hamiltonian (Abragam 1986), are shown as full

curves in figure 10. In table 2, the SHF and quadrupole data are given in terms of the isotropic SHF constants, the anisotropic SHF constants b and b' which are related to the SHF and quadrupole tensors, respectively, by

$$\mathbf{A} = a\mathbf{I} + \mathbf{B}$$
$$b = \tfrac{1}{2}B_{zz}$$
$$b' = \tfrac{1}{2}(B_{xx} - B_{yy})$$
$$q = \tfrac{1}{2}Q_{zz}$$
$$q' = \tfrac{1}{2}(Q_{xx} - Q_{yy}).$$

The orientation of each tensor is given by a set of Euler angles. The analysis of the spectra and the definition of the angles which determine the tensor orientation proceeded in a similar fashion to that described in detail in Bauer (1983) and Niklas (1983) for the two types of F centres in BaFCl.

4. Discussion

4.1. The optical properties of the F centres

A tetragonal crystal field acts on both types of F centre. The $F(F^-)$ centre has D_{2d} symmetry and the $F(Br^-)$ centre has C_{4v} symmetry. Both symmetries are isomorphous with respect to each other, therefore the following considerations apply for both centres. The ground state has approximately an s-like wavefunction and can be described by an A_1 state. The degeneracy of the excited P states is partly lifted by the crystal field. The excited states split into B_2 (p_z) and E (p_x, p_y) states. If the electrical vector $\boldsymbol{E}$ is perpendicular to the c-axis, only the transition $A_1 \rightarrow E$ can be induced. For $\boldsymbol{E} \parallel c$, only the transition $A_1 \rightarrow B_2$ is excited (Lemoyne 1975). From the optical data in table 1, the level scheme of figure 11 can be derived. The absorption of the $F(Br^-)$ centres for $\boldsymbol{E} \perp c$ peaks at about 2.15 eV. The E state reached is split by the electron–phonon coupling (Lemoyne 1975). The $A_1 \rightarrow B_2$ transition of the $F(Br^-)$ centre ($\boldsymbol{E} \parallel c$) has a photon energy of 2.58 eV. It follows that the E state is 2.15 eV above the ground state while the B_2 state is 0.43 eV above the E state. In the $F(F^-)$ centre, the energy positions of the E and B_2 states are interchanged. The E state is 2.65 eV above the ground state and 0.27 eV above the B_2 state.

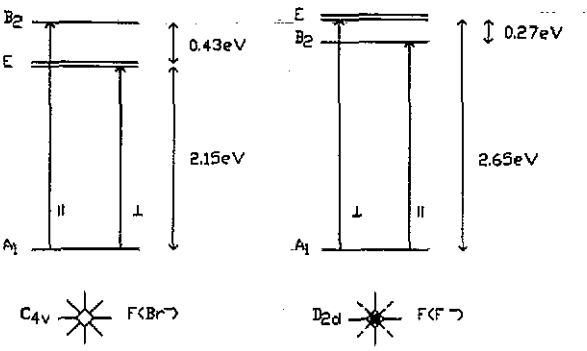

Figure 11. Schematic representation of the energy levels of $F(F^-)$ and $F(Br^-)$ in BaFBr.

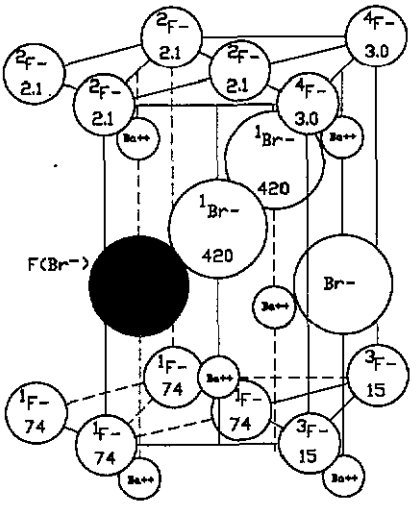

Figure 12. Spin density distribution for $F(Br^-)$ centres in 10^{-4} au^{-3}.

When analysing the MCDA spectra in the rigid shift approximation (Henry 1968) as was done previously for the F centres in alkali halides, for the spin–orbit splitting of the unrelaxed excited states one obtains 70 meV for the $F(Br^-)$ centre and 55 meV for the $F(F^-)$ centre. These spin–orbit interactions are responsible for splitting the absorption bands into two bands (figure 2), one being the transition to the $j = \frac{1}{2}$ the other to the $j = \frac{3}{2}$ excited states. The difference in the value of the spin–orbit splitting found from the MCDA compared with the absorption band splitting is similar to that found for F centres in CsBr. There it was ascribed to the effect of lattice vibrations which split the two states further than calculated from the spin–orbit interactions alone (Henry 1968). The MCDA of both the $F(Br^-)$ and $F(F^-)$ centres are non-symmetrical and broadened towards the high-energy side due to transitions to higher excited states, as demonstrated by the ODEPR tagging experiments. Such higher transitions were also observed for F centres in the alkali halides and called 'K-bands' (Fowler 1968). The consequence of this observation is that the optical excitation of $F(F^-)$ centres in their main absorption band at 2.65 eV for $\boldsymbol{E} \perp \boldsymbol{c}$ also excites the $F(Br^-)$ centres. This is an important observation since it implies that in the europium-doped storage phosphor, excitation in the $F(F^-)$ band causes the same photostimulation process as excitation in the $F(Br^-)$ band does, in contrast to some recent claims (Thoms 1991).

The luminesence experiments showed that $F(F^-)$ emission can be excited indirectly by irradiating in the $F(Br^-)$ absorption band for $\boldsymbol{E} \parallel \boldsymbol{c}$, and that the $F(Br^-)$ emission can be excited indirectly by irradiating in the $F(F^-)$ band for $\boldsymbol{E} \perp \boldsymbol{c}$. This means that one can always excite both emissions by irradiating in the high-energy band of one of the F centres. Since both F bands exchange the energy position of their absorption bands, for the two polarizations one can always excite both emissions by irradiating in the absorption band of one of the F centre types, depending on the choice of polarization. These emission properties can be explained by an energy transfer process between the two types of F centres, implying that there is a spatial correlation between them. The existence of such a correlation was also found from cross relaxation experiments (Koschnick 1992). Since there is no energy resonance

between emission and absorption, one must conclude that the energy transfer process between the two centres is radiationless. According to a simple dipole–dipole approximation, the probability for a radiationless energy transfer has a distance dependence of R^{-6} (Auzel 1980). Therefore, only centre pairs have an energy transfer, the separation of which is much smaller than the statistical separation which is about 200 Å for the concentrations of about 5×10^{16} cm^{-3}. It is interesting to note that the cross relaxation, as measured by the MCDA-ODEPR technique (Koschnick 1992) is also dependent upon R^{-6}. Thus, from two quite independent experiments, we have an indication that the F(Br$^-$) centres and F(F$^-$) centres are created with a spatial correlation by x-irradiation. (No such experiments could be done on the two types of F centre in additively coloured material because of our failure to produce sufficient F(F$^-$) centres by this method.) From our experiments, however, we cannot say what fraction of the two F centres are correlated.

4.2. The structures of the F(F$^-$) and F(Br$^-$) centres

From the angular dependence of the ODENDOR lines from F(Br$^-$), its identification could be made in a straightforward manner, whereas for the F(F$^-$) centre the absence of an angular dependence makes identification more difficult. The optical absorption bands and the MCDA which we have assigned to the F(F$^-$) centres also appear, albeit weakly, in additively coloured crystals. The g factor of 2.0 is typical for F centres. A comparison of the optical absorption bands and their dependence on the polarization with those found for F(F$^-$) centres in BaFCl and unambiguously identified by ENDOR (Yuste 1976, Bauer 1983) shows a strong similarity to those found here. The positions of the bands are just shifted by a few hundred meV on going from BaFCl to BaFBr.

From the SHF interactions measured by ENDOR for the F(Br$^-$) centre, one can calculate the unpaired spin density, $|\Psi|^2$, at the ligands using the well known relation for the isotropic SHF constant (Slichter 1980):

$$a = \tfrac{2}{3}\mu_0 g_I \mu_n g_e \mu_B |\Psi(0)|^2.$$

Figure 1 shows that the spin density distribution is anisotropic. At the site of the second-shell fluorine nuclei it is lower than at the third- and fourth-shell fluorine nuclei. This indicates a spin transfer mechanism due to the mutual overlap between adjacent lattice ions which was also found for the F(Cl$^-$) centre in BaFCl (Bauer 1983). Following the procedures developed to explain the SHF interactions of F centres in alkali halides, according to which an envelope function is orthogonalized to the cores of the ligand ions (Gourary 1960) we have tried in a simple approximation to determine an envelope function of the 1s type:

$$\Phi = \frac{1}{\sqrt{\pi}} a^{3/2} \exp(-ar).$$

By taking $a = 0.65$ au^{-1}, we could give a good explanation of the isotropic SHF constants of the nearest fluorine and bromine neighbours. (For the lattice ions, we used the free ion orbitals.) However, this envelope function is too simple to be able to explain the SHF data at the other ligands satisfactorily. We did not attempt to develop more detailed theoretical models.

5. Conclusions

From the polarization dependence of the spectral positions of the F centre absorption bands and the fact that they have transitions to higher excited states, it is clear that when using BaFBr powders as phosphor storage material one always excites both types of F centre in any read-out procedure. This should be taken into account when arriving at any conclusions about which centres participate in the photostimulated luminescence mechanism responsible for the read-out of the stored image. In our opinion, a recent paper on this subject needs revision since the optical properties of the F centres were not taken into account correctly (Thoms 1991).

The reason why a proportion of the $F(F^-)$ and $F(Br^-)$ centres produced by x-irradiation are spatially correlated is not clear at this time. It may be related to the mechanism by which $F(Br^-)$ centres are produced, which is controlled by the presence of oxide impurities, as is discussed in more detail by Koschnick *et al* (1992).

Acknowledgments

One of the authors (FKK) would like to thank the Eastman Kodak Company for their generous financial support of this project, and Drs W G McDugle and R H Nuttall for general discussions during the course of this work.

References

Abragam A and Bleaney B 1986 *Electron Paramagnetic Resonance of Transition Ions* (New York: Dover)
Ahlers F J, Lohse F, Spaeth J-M and Mollenauer L F 1983 *Phys. Rev.* B **28** 1249
Auzel F 1980 *Radiationless Processes* ed B DiBartolo (New York: Plenum) S 213
Bauer R U, Niklas J R and Spaeth J-M 1983 *Phys. Status Solidi* b **118** 557
Beck H P 1979 *Z. Anorg. Chem.* **451** 73
Bromba M U A and Ziegler H 1979 *Anal. Chem.* **51** 1760
Fowler W B 1968 *Physics of Color Centers* ed W B Fowler (New York: Academic)
Gourary R S and Adrian F J 1960 *Solid State Physics* vol 10 (New York: Academic) p 127
Henry H Ch and Slichter Ch P 1968 *Physics of Color Centers* ed W B Fowler (New York: Academic)
Hoentzsch Ch, Niklas J R and Spaeth J-M 1978 *Rev. Sci. Instrum.* **49** 1100
Hofmann D M, Meyer B K, Lohse F and Spaeth J-M 1984 *Phys. Rev. Lett.* **53** 1187
Koschnick F K, Spaeth J-M and Eachus R S 1992 *J. Phys.: Condens. Matter* **4** 3015
Lemoyne D, Duran J, Yuste M and Billardon M 1975 *J. Phys. C: Solid State Phys.* **8** 1455
Liebig B W and Nicollin D 1977 *Acta Crystallogr.* B **33** 2790
Luty F and Mort J 1964 *Phys. Rev. Lett.* **12** 45
Niklas J R, Bauer R U and Spaeth J-M 1983 *Phys. Status Solidi* b **119** 171
Seidel H and Wolf H C 1986 *Physics of Color Centers* ed W B Fowler (New York: Academic)
Slichter Ch P 1980 *Principles of Magnetic Resonance* (Berlin: Springer)
Sonoda M, Takano M, Miyahara J and Kato H 1983 *Radiology* **148** 835
Takahashi K, Miyahara J and Shibahara Y 1985 *J. Electrochem. Soc.* **132** 1492
Thoms M, von Seggern H and Winnacker A 1991 *Phys. Rev.* B **44** 9240
van Doorn C Z 1961 *Rev. Sci. Instrum.* **32** 755
von Seggern H, Voigt T, Knupfer W and Lange G 1988a *J. Appl. Phys.* **64** 1405
von Seggern H, Voigt T and Schwarzmichel K 1988b *Siemens Forsch.-u. Entwickl.-Ber.* **17** 120
Yuste M, Taurel L, Rahmani M and Lemoyne D 1976 *J. Phys. Chem. Sol.* **37** 961
Ziegler H 1981 *Appl. Spectrosc.* **35** 88